Easy-separable magnetic nanoparticle-supported Pd catalysts: Kinetics, stability and catalyst re-use

Urszula Laska [a,b], Christopher G. Frost [b], Gareth J. Price [b], Pawel K. Plucinski [a,*]

[a] Department of Chemical Engineering, University of Bath, Claverton Down, Bath BA2 7AY, UK
[b] Department of Chemistry, University of Bath, Claverton Down, Bath BA2 7AY, UK

ARTICLE INFO

ABSTRACT

A series of novel palladium-based catalysts supported on magnetic nanoparticles with diameters of 7–17 nm have been prepared and evaluated in C–C coupling, hydrogenation and amination reactions. One type of catalyst used palladium complexes containing phosphine and/or acetate ligands for applications in Suzuki and Heck reactions. The second type consisted of Pd(0)-functionalised magnetic cores for use in hydrogenation and C–C coupling. Each type was effective for a range of reactions and was easily recoverable from the reaction mixture due to the superparamagnetic behaviour of the support. Detailed rate studies, found to correspond to pseudo-first-order kinetics, were conducted to assist in determining the mechanism of the reactions and showed that, during Heck reactions, Pd leaching is critically dependent on the presence of the aryl halide. The catalysts were found to retain their activity for several cycles although the rate of reaction was markedly reduced on re-use.

1. Introduction

In recent years, the design of efficient and recoverable catalysts has become an important issue for reasons of economic and environmental impact. One strategy has focused on combining the advantages of different types of catalyst; for example the high activity and selectivity of homogeneous species with the ease of separation and recycling of heterogeneous catalysts. A number of approaches have been reported [1] including biphasic systems [1], polymer or membrane supports [1,2] and dendrimers [3]. In this regard, the use of superparamagnetic nanoparticles (MNPs) as catalyst carriers is very promising due to their large surface area, straightforward and relatively low-cost preparation and low toxicity [4]. Mainly though, they can be readily dispersed throughout reaction media but separation at the end of the reaction is facilitated by their attraction to a magnetic field [4].

Recently, a number of functionalised MNPs have been employed in a range of organic transformations, showing excellent catalytic activities in C–C coupling [5], hydrogenation [6], oxidation [7], amination [8] and nitrile hydration [9] reactions. Most required specific functionalisation procedures to anchor the catalytically active complexes onto the MNP surface. Previous work in our group showed that C–C coupling and hydrogenation reactions were effi-

ciently catalysed by rhodium species immobilised on MNPs [10]. In continuation of our work on MNP-based catalysts, we report here a straightforward preparation of MNP-supported palladium catalysts and their use in C–C bond forming reactions and selective hydrogenations.

In general, the most important aspect of catalyst application is its efficiency in terms of the reaction rate and yield as well as its capacity to be recycled. Although Pd-bearing MNP catalysts have been reported previously, [5,6,8] there is limited evidence of how the activity changes over several catalyst recycles. To the best of our knowledge this is the first report describing a detailed kinetic study. Surprisingly, although many MNP-supported systems have been studied, little attention has been paid to the real nature of the catalytic species taking part in the reaction. Thus, in addition to detailed investigations of the reactivity, efficiency and stability of three palladium MNP-based catalysts, we investigate this aspect of the catalytic processes.

2. Experimental

2.1. Materials and instrumentation

All chemicals were of analytical grade or better. Methanol and dichloromethane were purified and dried using standard procedures. All the remaining reagents and chemicals were used as received. Sodium 3-(diphenylphosphino)benzenesulfonate (TPPMS)

* Corresponding author.
  E-mail address: p.plucinski@bath.ac.uk (P.K. Plucinski).

was synthesised as described previously [10,11]. Pd(TPPMS)$_2$Cl$_2$ was prepared by treatment of TPPMS with PdCl$_2$ (2:1.1 M ratio, respectively) in dry THF at room temperature for 24 h. The synthesised Pd(TPPMS)$_2$Cl$_2$ was immobilised onto MNPs without further purification.

The size and morphology of the MNPs were characterised by transmission electron microscopy. Low-resolution TEM images were recorded on JEOL JEM-1200EX II Transmission Electron Microscope (JEOL, Tokyo, Japan) equipped with a Gatan Dualvision Digital Camera and Digital Micrograph 3.4 Software (Gatan, Oxon, UK). High-resolution HRTEM images were obtained using a JEOL JEM 2010 with LaB6-Cathode and CCD-Camera (TVIPS). EDX patterns were recorded on a JEOL JSM 5900 LV with a tungsten cathode. Powder X-ray diffraction (XRD) data were obtained using a Philips 4 kW X-ray generator (PW1730) with a Cu KM X-ray source (N = 1.54060 Å) and a diffractometer goniometer (PW1820) controlled via Philips (PW1877 PC-APD) software. The palladium contents in supernatants were determined by atomic absorption spectrophotometry (AAS) using standard methods with a Varian AA 275 atomic absorption spectrophotometer. Gas chromatography analyses were carried out on an Agilent Technologies 6890 N Network GC System equipped with a HP-5 column 30 m × 0.320 mm. NMR spectra were obtained in CDCl$_3$ on a Bruker Avance 300 spectrometer operating at 300 MHz. IR spectra (4000–400 cm^{-1}) were recorded as KBr discs on a Nicolet Nexus FT-IR spectrometer.

2.2. Catalyst preparation

The iron oxide magnetic support was prepared by co-precipitation of ferric and ferrous ions in a basic solution, using a slight modification of the method described by Lyon et al. [12]. The appropriate amount of catalyst precursor, Pd(OAc)$_2$ (0.12–0.36 mmol) or Pd(TPP)$_2$(OAc)$_2$ (90 mg, 0.12 mmol), and dry MNPs (2.0 g) were placed into a flask. Following purging with N$_2$ for 15 min, 20 mL of dry methanol was added via a syringe and the mixture was subjected to ultrasonication using a 30 kHz, 50 W cleaning bath. The solid catalyst was separated using an external permanent magnet and was washed several times with dry methanol. The catalyst loading was calculated from a material balance including the analytical results from supernatant and washing solutions. Three consecutive washings were sufficient to remove the non-immobilised Pd complexes.

The modified iterative seeding procedure described by Lyon et al. [12] was used for the preparation of MNP-Pd(0) using 0.2 mM of H$_2$PdCl$_4$ as the metal source and 0.2 M of NaBH$_4$ as the reducing agent.

2.3. Procedures for catalytic reactions

2.3.1. Heck coupling reactions

In the reaction flask (Carousel 12 Reaction Station, Radleys Discovery Technologies, UK), olefin (0.60 mmol), aryl bromide (0.50 mmol) and potassium acetate (98.1 mg, 1.00 mmol) were placed. 10 mL of N-methyl-2-pyrrolidone (NMP) and the catalyst were added (catalyst concentration in the range between 1.25 and 7.5 mol% of Pd in respect to aryl bromide) and the reaction mixture was stirred under reflux at 130 °C. Aliquots of the reaction mixture were taken at time intervals and were analysed by gas chromatography after catalyst removal. After completion, the reaction mixture was cooled in an ice bath, separated by magnetic decantation, poured into water (40 mL) and extracted with toluene (3 × 30 mL). The collected organic layers and washing supernatants were washed with water (30 mL) and brine (30 mL) then dried over MgSO$_4$. After filtration, the solvents were evaporated under vacuum and the products were analysed using ^{1}H NMR

and gas chromatography. Nanoparticle-supported catalyst was washed with NMP (2 × 5 mL) and toluene (2 × 5 mL), dried under N$_2$ and used for subsequent reaction.

2.3.2. Suzuki–Miyaura coupling reactions

The reaction flask was charged with phenylboronic acid (67.1 mg, 0.55 mmol), aryl bromide (0.50 mmol) and potassium acetate (128 mg, 1.30 mmol). After the addition of 10 mL of N,N-dimethyl formamide (DMF) and the catalyst (5 mol% of Pd in respect to aryl bromide), the reaction mixture was stirred under reflux at 50 °C for 24 h. After cooling, the reaction mixture was separated using an external permanent magnet. The product mixture was poured into diethyl ether (20 mL), washed with water and the product was extracted with diethyl ether (3 × 20 mL) and dried over Na$_2$SO$_4$. After filtration the samples were analysed using gas chromatography.

2.3.3. Hydrogenation of benzaldehyde and dimethyl itaconate

Hydrogenation of benzaldehyde was carried out in a 50 mL high-pressure glass-lined stainless steel reactor. The reactor was charged with benzaldehyde (0.531 g, 5.0 mmol), MNP-Pd(0) catalyst (5 mol% Pd) and 25 mL of 2-propanol and was then sealed. It was alternatively purged with N$_2$ and H$_2$ four times and was finally filled with H$_2$ to a pressure of 3 bar. The reaction mixture was stirred at 50 °C for 4 h. The reactor was cooled to room temperature, depressurized and the catalyst was separated by magnetic decantation and washed three times with 2-propanol. The reaction mixture and supernatants were collected and the solvent was evaporated. The samples were analysed with gas chromatography and the final product structure was confirmed by ^{1}H NMR.

For the hydrogenation of dimethyl itaconate, a similar procedure was used. MNP-Pd(0) catalyst (1 mol% Pd), dimethyl itaconate (0.063 g, 0.4 mmol) and 20 mL of dry MeOH were loaded into the reactor, following by flushing the system with N$_2$ and H$_2$ and finally filling with H$_2$ (4 bar). The reaction mixture was stirred at 50 °C.

2.3.4. Amination of bromobenzene

An oven-dried flask was charged with catalyst (5 mol% of Pd in respect to bromobenzene), NaO^{t}Bu (72.1 mg, 0.75 mmol) and ligand (1:2 Pd/ligand molar ratio). The tube was sealed, evacuated and back-filled with Ar. Dry toluene (10 mL) was added and the mixture was heated at 80 °C with stirring for 30 min. Bromobenzene (78.5 mg, 0.5 mmol) and morpholine (52.3 mg, 0.6 mmol) were added via a syringe and the reaction mixture was stirred at 80 °C for a further 24 h. The products were analysed using gas chromatography and ^{1}H NMR spectroscopy. For the amination reactions, the experimental results are shown as yield (based on the product concentrations); in all other cases the results are shown as conversions (based on reactant concentrations).

2.4. Homogeneity test

The nature of the catalytic species was investigated by a catalyst poisoning study. A microporous resin (400–600 μm particle size) Quadrapure™ TU [13] was used as a Pd scavenger. Double the amount of thiourea (TU) scavenging groups required for a complete coordination of the Pd was used in each experiment.

3. Results and discussion

3.1. Catalyst preparation and characterisation

In our initial screening studies, the iron oxide MNPs were functionalised in a simple one-step procedure using commercially available palladium(II) acetate (Pd(OAc)$_2$) or bis(triphenylphos-

phine)palladium(II) diacetate ($Pd(TPP)_2(OAc)_2$) (Scheme 1). Atomic absorption spectrophotometry (AAS) confirmed loadings of ca. 0.06–0.18 and 0.06 mmol of Pd per gram of MNP-[$Pd(OAc)_2$] and MNP-[$Pd(TPP)_2(OAc)_2$] catalysts, respectively. Palladium acetate adsorbed quantitatively on the iron oxide MNPs. AAS measurements showed that no Pd remained in the supernatant when using $Pd(OAc)_2$ (within the detection limit of ca. 0.1 ppm Pd) indicating very strong adsorption on the surface of the MNPs. With the more sterically demanding $Pd(TPP)_2(OAc)_2$, the adsorption was weaker and the palladium was present in the supernatant after magnetic separation although three repeated washings were sufficient to remove the excess of $Pd(TPP)_2(OAc)_2$.

In the second approach, the iron oxide nanoparticles were functionalised with metallic Pd(0) by reducing Pd^{2+} ions (yielding (MNP-Pd(0)) using a modification of the iterative seeding method [12]. AAS analysis gave a catalyst loading of ca. 1.0 mmol Pd per g of MNP.

The size of the synthesised nanoparticles ranged from 7 to 17 nm, with average 8 ± 2 nm (in most cases) as based on TEM, XRD (Debye–Scherrer formula [14]) and superconducting quantum interference device (SQUID) measurements (Langevin equation). Particles deviated from sphericity, due to the spinel nature of mag-

netite. XRD confirmed the crystalline nature of the MNPs and the peaks corresponded well to the standard magnetite reflections. The crystalline structure did not change after the immobilisation of organometallic species although the presence of metallic Pd in the MNP-Pd(0) system can be clearly seen (Fig. 1). Magnetisation curves (Fig. 2) obtained by SQUID showed typical characteristics of superparamagnetic behaviour for all MNP samples; zero coercivity and no remanence on hysteresis. In all cases, the separation of the catalyst was achieved by applying an external permanent magnet, making the recovery of the catalyst very straightforward. These methods have their limitations [15]; however, the good agreement of the average sizes measured by all three methods (TEM, XRD and SQUID) supports the validity of the quoted values.

3.2. Initial screening of catalytic performance

The MNP-supported catalysts were tested for activity in the Heck cross-coupling reaction of styrene with 4-bromonitrobenzene (Table 1, entries 1–3) as well as in a Suzuki coupling between phenylboronic acid and bromobenzene (Table 1, entries 5–7). All the systems studied were highly efficient in the Heck reaction although rather less so for the Suzuki reactions. Most significantly, reactions with unfunctionalised MNPs afforded none of the expected product, confirming the role of Pd in the catalysis (Table 1, entries 4 and 8). In these initial experiments a relatively high level of 5 mol% of the reactant/active metal ratio was employed to give short reaction times although, as shown below, more typical
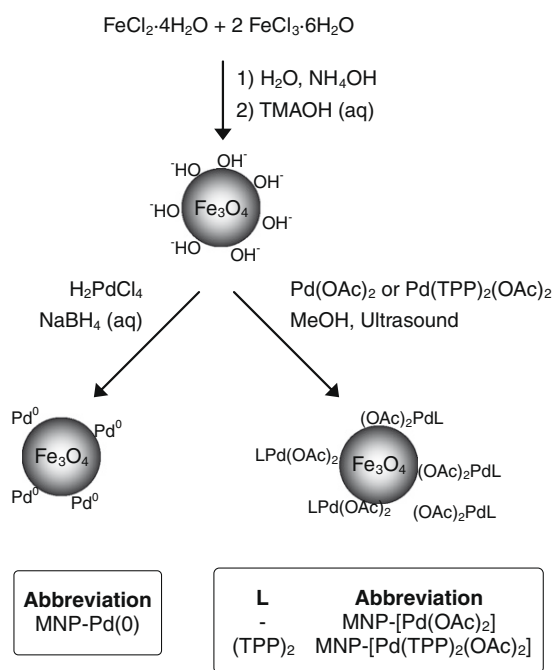
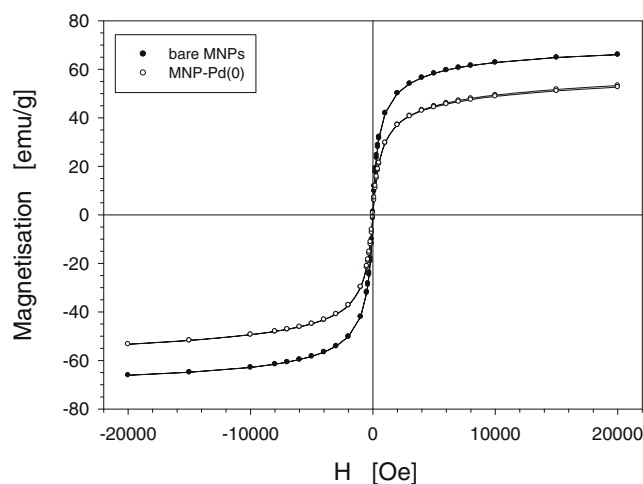**Scheme 1.** The preparation of MNP-supported palladium catalysts.

Fig. 2. SQUID magnetisation curves of bare and Pd(0)-bearing nanoparticles. The values for the Pd-coated MNP refer to per gram of iron oxide.
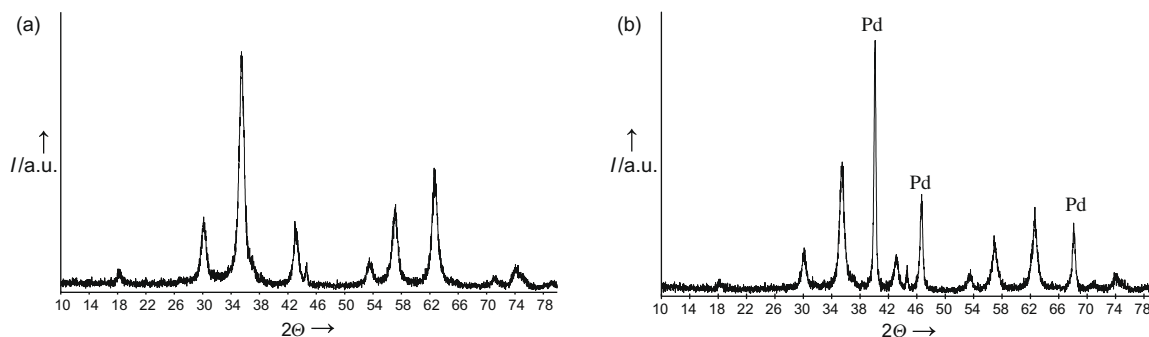

Fig. 1. XRD patterns for MNP-based Pd catalysts: (a) bare NPs; (b) MNP-Pd(0) (ca. 1 mmol Pd per g of MNPs).

Table 1
C–C coupling reactions catalysed by MNP-supported Pd.

Entry	Catalyst	Conversion (%)[a]
Heck coupling		
1	MNP-[Pd(OAc)₂]	100
2	MNP-[Pd(TPP)₂(OAc)₂]	>99
3	MNP-Pd(0)	>99
4	Bare MNP	0
Suzuki coupling		
5	MNP-[Pd(OAc)₂]	85
6	MNP-[Pd(TPP)₂(OAc)₂]	45
7	MNP-Pd(0)	54
8	Bare MNP	0

[a] Determined by gas chromatography.

levels of Pd [16,17], are also effective, albeit at the expense of longer reaction times.

Given its higher efficiency in these reactions as well as the environmental advantage of being phosphine-free, MNP-[Pd(OAc)₂] was chosen for further study. A range of substituted aryl bromides were investigated to determine the scope and limitations in Heck reactions of styrene and of *n*-butyl acrylate (Fig. 3). A range of activities were observed from 10% to 100% conversions depending on the nature of aryl bromide. For both styrene and *n*-butyl acrylate, the fastest kinetics were observed for 4-bromonitrobenzene (**5**), 4-bromobenzaldehyde (**2**) and 2-bromobenzaldehyde (**3**); the slowest kinetics were observed for bromobenzene (**1**). This shows that electron-withdrawing substituents [18] enhance the coupling product formation, while electron-donating groups [18] have a negative influence on the process kinetics.

Similar kinetics for (**2**), (**3**) and (**5**) could suggest that the kinetics are limited by mass transfer and diffusion of the MNPs. To investigate this, the detailed reaction kinetics were measured as a function of temperature between 100 and 160 °C for a selection of aryl bromides: two from the group with highest rates ((**2**) and (**5**)) and two from the group with slowest rates ((**1**) and (**7**)). Each of the reactions displayed first-order kinetics, and rate constants and activation energies (Table 2) were calculated using the standard procedures [19]. For both groups of aryl bromides, high activation energies (ca. 62–91 kJ mol⁻¹) were found indicating that the reactions were not diffusion limited but are influenced by the chemical nature of the aryl bromide. Since an oxidative addition of palladium species to aryl bromide is the rate-limiting step of Heck coupling [20], it follows that faster addition is associated with the presence of electron-withdrawing substituents. As expected, the highest value was observed for 4-bromonitrobenzene, **5** which has the strongest electron-withdrawing substituent.

The activity of the MNP-[Pd(OAc)₂] catalysts was further explored in the Suzuki reaction of phenylboronic acid and various aryl bromides. Each of the aryl bromides studied underwent reaction with excellent conversions of 97–100% to the expected product (see Table 3).

After each reaction, the catalyst separation was easily achieved by applying an external magnetic field (surface magnetisation 0.3 T). The most significant advantage of the magnetic catalytic systems used is this simple catalyst separation. More than 99 wt.% of MNPs were recovered after washing three times with NMP (based on AAS analysis of Fe and Pd). Cumulative AAS analyses of cold post-reaction supernatant and five consecutive wash solutions showed that only ca. 1% of initial amounts of Fe and Pd was lost during this process, proving the efficiency of magnetic
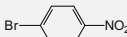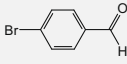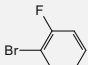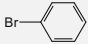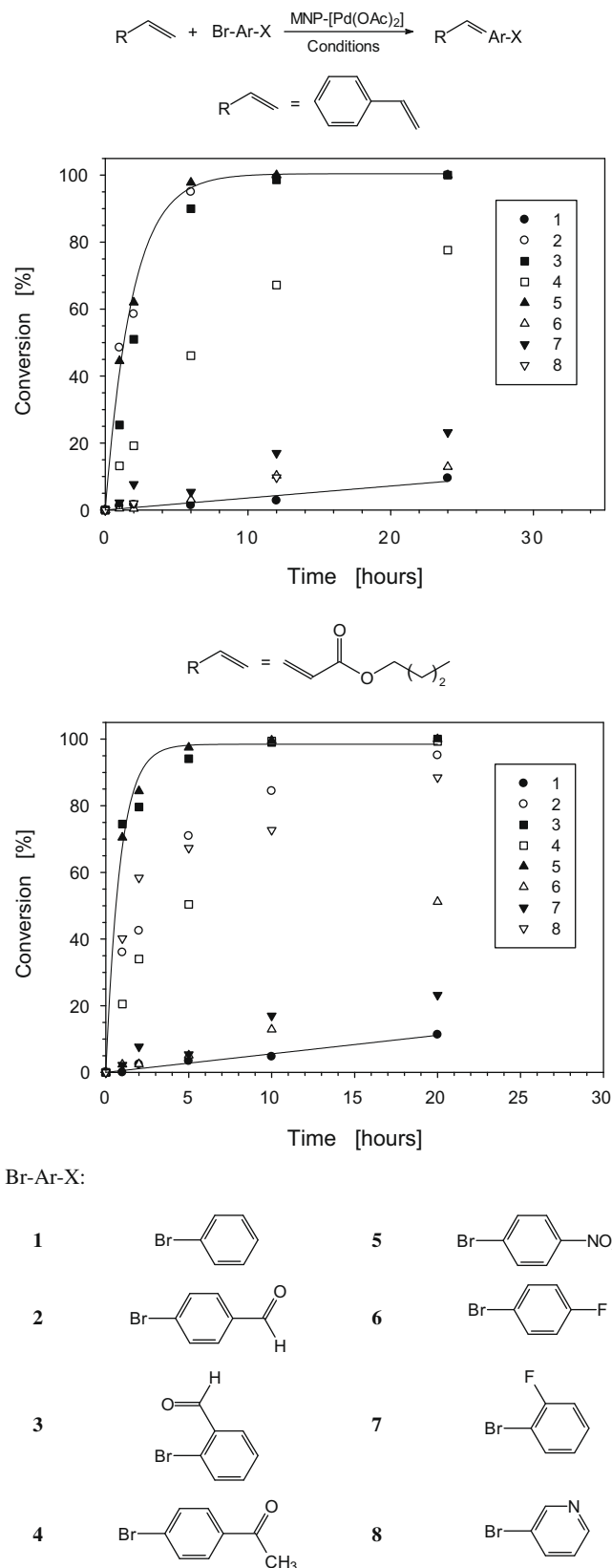
Fig. 3. The kinetics of Heck reactions catalysed by MNP-[Pd(OAc)₂] using styrene or *n*-butyl acrylate. Reaction conditions: 1.0 eq. Br–Ar-X, 1.2 eq. olefin, 2.0 eq. KOAc, 5 mol% Pd, 10 mL NMP, 130 °C.
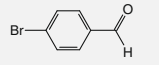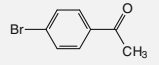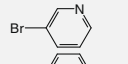
separation. The recycled catalysts were used for several repeat reactions without loss (in most cases) of catalytic activity as shown

Table 2
Heck cross-coupling reactions catalysed by NP-[Pd(OAc)$_2$].[a]

Entry	Br–Ar-X	E_A (kJ mol^{-1})
1	Br—⬡—NO$_2$	90.7
2	Br—⬡—C(=O)H	79.9
3	(F, Br-substituted benzene)	69.3
4	Br—⬡	60.8

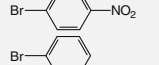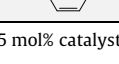[a] Reaction conditions: 1.0 eq. Br–Ar-X, 1.2 eq. olefin, 2.0 eq. KOAc, 5 mol% Pd, 10 mL NMP, 130 °C.

Table 3
Suzuki cross-coupling reactions catalysed by MNP-[Pd(OAc)$_2$].[a]

⬡—B(OH)$_2$ + Br—⬡—Ar-X →(MNP-[Pd(OAc)$_2$], Conditions) ⬡—⬡—Ar-X

Entry	Br–Ar-X	Conversion (%)[b]
1	Br—⬡—C(=O)H	100.0
2	Br—⬡—C(=O)CH$_3$	99
3	Br—(pyridine, N)	99
4	Br—⬡—NO$_2$	97
5	Br—⬡	85

[a] Reaction conditions: 5 mol% catalyst based on Pd, DMF, KOAc, 100 °C, reaction time = 24 h.
[b] Determined by gas chromatography.

in Table 4. High activity is retained for MNP-[Pd(OAc)$_2$] and MNP-Pd(0). With MNP-[Pd(TPP)$_2$(OAc)$_2$], the conversion decreased markedly after the second run. This can be explained by TEM analysis which shows that the MNP-[Pd(TPP)$_2$(OAc)$_2$] agglomerated (Fig. 4a and b) during the reaction which would lead to lower availability of catalytic sites. No such changes in nanoparticle dispersion were observed in the case of MNP-[Pd(OAc)$_2$] or MNP-Pd(0) catalyst after re-use (Fig. 4c and d), suggesting that the triphenylphosphine groups may promote agglomeration in polar solvent such as NMP by interparticle interactions.

Having demonstrated that iron oxide-supported Pd catalysts were highly effective for carbon–carbon coupling reactions, the

Table 4
Recycling of magnetic nanoparticle-supported Pd catalysts.

⬡—CH=CH$_2$ + Br—⬡—NO$_2$ →(MNP-Pd cat. (5 mol% Pd), NMP, KOAc, 130 °C) ⬡—CH=CH—⬡—NO$_2$

Entry	Catalyst	Reaction cycle	Conversion (%)[a]
1	MNP-[Pd(OAc)$_2$]	I	100
		II	100
		III	99
		IV	99
2	MNP-[Pd(TPP)$_2$(OAc)$_2$]	I	100
		II	91
		III	12
3	MNP-Pd(0)	I	100
		II	>99
		III	>99

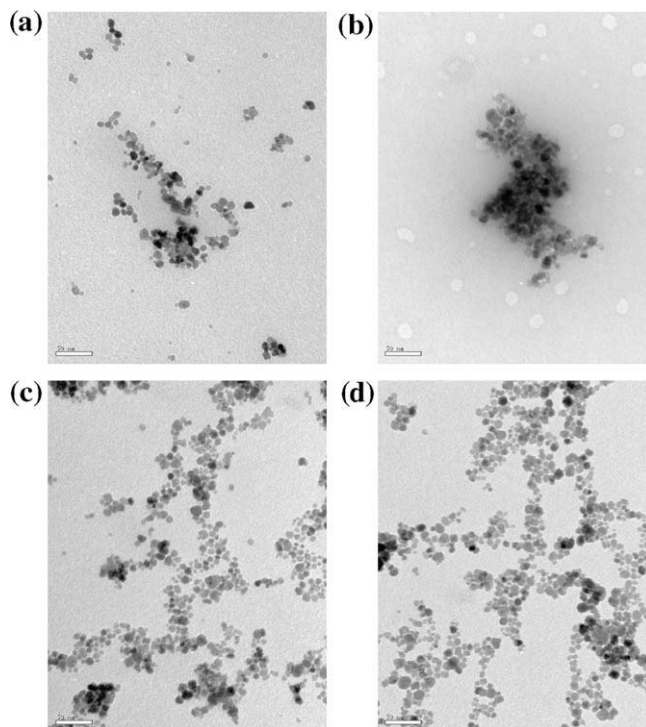[a] Determined by gas chromatography.

Fig. 4. TEM images of MNP-[Pd(TPP)$_2$(OAc)$_2$]: (a) before and (b) after the reaction, and MNP-[Pd(OAc)$_2$] (c) before and (d) after reaction. The scale bar represents 50 nm.

activity of the ligand-free MNP-Pd(0) in the hydrogenation reaction was investigated as a model of a multi-phase (gas/liquid) process. For a hydrogen partial pressure, p_{H_2}, of 1 bar, MNP-Pd(0) gave a complete hydrogenation of benzaldehyde to benzyl alcohol in 4 h with 100% selectivity for the C=O group over the aromatic ring. No ring hydrogenation products were observed under these conditions. An increase to p_{H_2} = 2 bar accelerated the reaction, giving quantitative hydrogenation within 1 h (Fig. 5). Further increase to p_{H_2} = 3 bar increased the rate of hydrogenation although increasing the pressure above this gave no further increase in rate suggesting that the catalytic sites were saturated. Measuring the reaction rate of benzaldehyde hydrogenation over the range of 40–70 °C gave an activation energy of 66.1 kJ mol^{-1}.

The MNP-Pd(0) system was also shown to be very effective in catalysing the hydrogenation of olefinic C=C double bonds. Using dimethyl itaconate as an example, complete conversion was observed within 4 min when 1 mol% of Pd (relative to substrate) was used (p_{H_2} = 4 bar, T = 50 °C). The efficiency of the catalyst is demonstrated by the result that a complete conversion could be obtained in 10 min with only 0.5 mol% Pd loading.

The results discussed above prompted us to screen the catalysts for reactivity in the amination of aryl halides, a very useful organic transformation for C–N bond formation [21]. However, the MNP-supported Pd systems were less satisfactory in catalysing the reaction between morpholine and bromobenzene. Each of the three palladium catalysts was used with NaO^{t}Bu as a standard base for the amination of aryl halides [21]. Unfortunately, the yields were very low (Table 5, entries 4–6) and in order to obtain higher conversion the use of supporting bulky electron-rich ligands such as 2-dicyclohexylphosphino-2′-(N,N-dimethylamino)biphenyl (DavePhos) and ethylenebis(diphenylphosphine) (DPPE) was necessary (Table 5, entries 1 and 2). With DavePhos as the homogeneous ligand the reaction occurred with similar yields of 42.5% and 39.9% after 24 h for MNP-Pd(0) and MNP-[Pd(OAc)$_2$], respectively. However, DPPE was ineffective for this
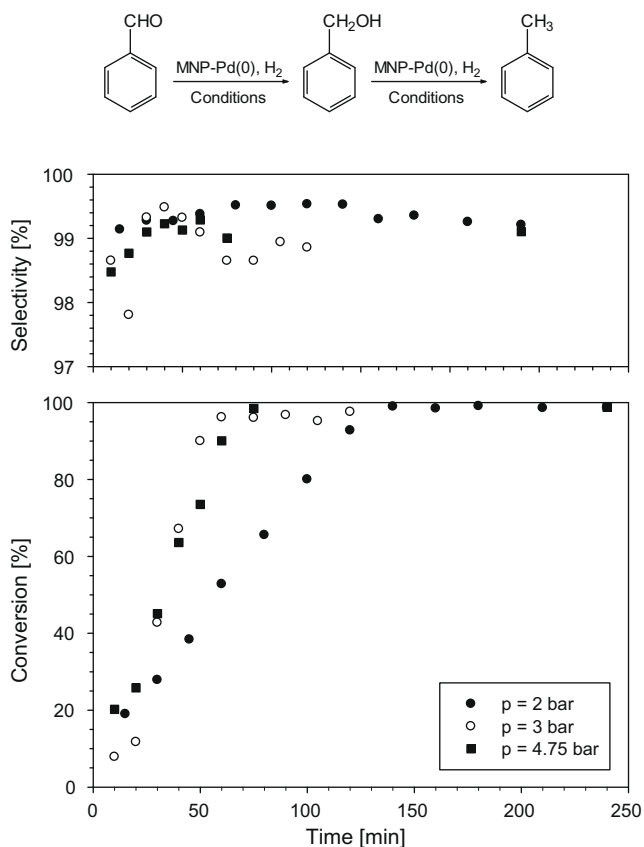
Fig. 5. Kinetic results (conversion and selectivity towards benzyl alcohol) for the hydrogenation of benzaldehyde catalysed by MNP-Pd(0) at 50 °C.

Table 5
Results for the amination of bromobenzene with morpholine[a] using various MNP-based catalytic systems.

Entry	Catalytic system	Homogeneous ligand	Yield (%)[b]
1	Pd(0)@MNP	DavePhos	42
2	MNP-[Pd(OAc)$_2$]	DavePhos	40
3	MNP-[Pd(OAc)$_2$]	DPPE	0
4	MNP-[Pd(OAc)$_2$]	–	0
5	MNP-[Pd(TPP)$_2$(OAc)$_2$]	–	<1
6	MNP-[Pd(TPPMS)$_2$Cl$_2$]	–	4

[a] Reaction conditions: 0.50 mmol bromobenzene, 0.60 mmol morpholine, 0.75 mmol NaO^{t}Bu, 5 mol% Pd, 10 mL of toluene under argon atmosphere, 24 h.
[b] Determined by GC and ^{1}H NMR spectroscopy.

process, giving a complex mixture containing none of the desired product.

The major factor inhibiting the MNP catalyst performance was the strong adsorption of the amine onto the nanoparticle surface. Comparative IR analysis showed absorptions at 1156 cm^{-1} (C–N stretching) as well as 1340 and 855 cm^{-1} (N–H bending) in the MNPs recovered after reaction, none of which was present in the unused catalysts. This suggests that there is a significant reactant inhibition of catalysts, which could be avoided by using sterically demanding ligands such as glutathione [22].

3.2.1. Homogeneous or heterogeneous catalysis?

In order to clarify whether the nature of the Pd species is involved in catalysis, a series of Heck reactions was carried out in

the presence of Quadrapure™ TU scavenger resin, which contains thiourea moieties with very high affinity for active palladium in homogeneous solution, [13]. Each of the three MNP-palladium catalysts was used while adding the scavenger at the start of the reaction or adding after 40 min reaction time (which for standard MNP-[Pd(OAc)$_2$] catalysts corresponded to ca. 35% conversion) and comparing with the results in the absence of the scavenger.

Examination of the kinetic profiles in Fig. 6 shows that in each case, addition of the scavenger had an effect on the reaction progress. The MNP-Pd(0) catalyst (Fig. 6a) was least affected; the initial rates of reaction were similar even where the Quadrapure TU was added at the start of the reaction. Moreover, addition after 40 min had little effect on the rate although the final conversion
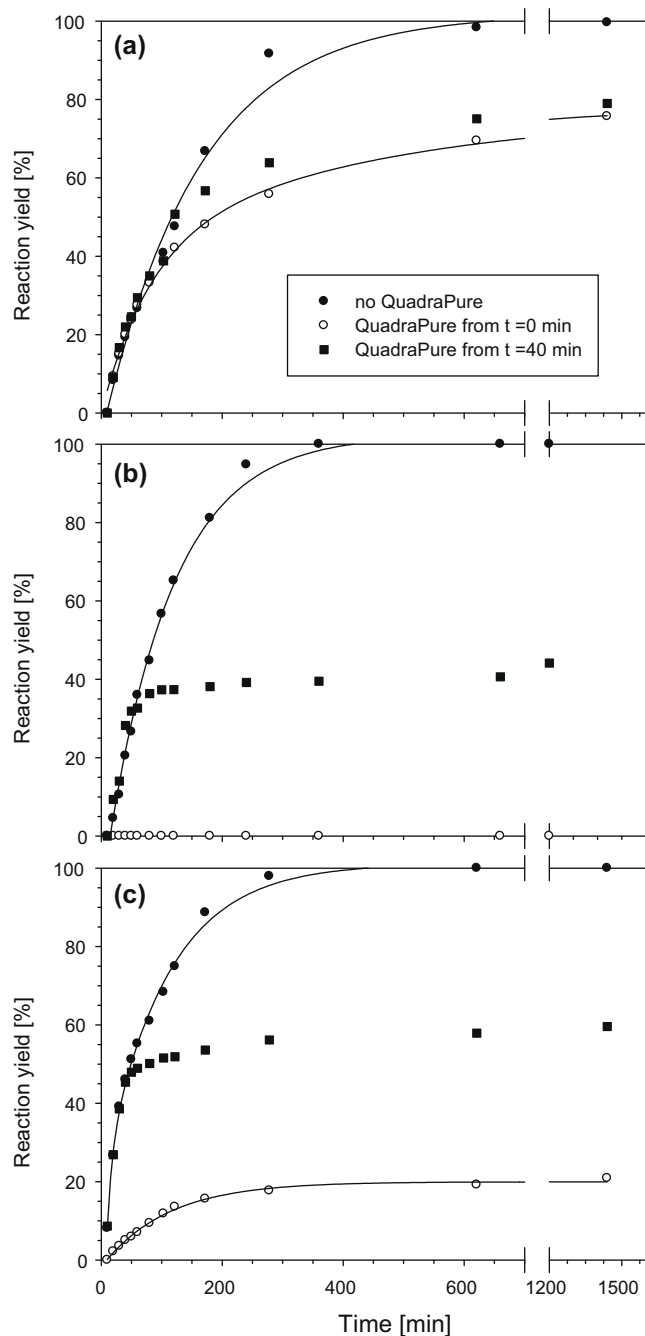

Fig. 6. Kinetic profiles for Heck reactions catalysed by MNP-based catalysts in the presence of a metal scavenger: (a) MNP-Pd(0), (b) MNP-[Pd(OAc)$_2$] and (c) MNP-[Pd(TPP)$_2$(OAc)$_2$].

achieved was reduced. This can be regarded as evidence of stable Pd(0) species on the MNP surface. The decrease of the final conversion may be attributed to the inclusion of MNPs inside the microporous scavenger resin. This was confirmed visually since, after reaction, resin pellets could be attracted by a magnetic field, whereas new Quadrapure TU resin showed no magnetic properties.

The observed catalytic behaviour of Pd immobilised on MNPs differs from that reported for Pd/C or for Pd supported on macroscopic oxides. Richardson and Jones, investigating the Heck coupling of iodoarenes with n-butyl acrylate, found that the addition of Quadrapure TU to the reacting mixture completely suppressed the reaction [23]. Considering the generally accepted mechanism of Heck coupling [24] which involves the presence of catalytically active soluble palladium species in solution, our results suggest a different mechanism for our catalyst, not involving a release and capture mechanism. The mechanistic aspects of our reactions need further investigations but it may be that coupling follows a "classical" Langmuir–Hinshelwood mechanism at the surface.

The other two systems, MNP-[Pd(OAc)$_2$] and MNP-[Pd(TPP)$_2$(OAc)$_2$] showed different behaviours. The addition of scavenger to MNP-[Pd(OAc)$_2$] stopped the reaction immediately on addition (Fig. 6b). For MNP-[Pd(TPP)$_2$(OAc)$_2$], the addition of scavenger considerably slowed down the reaction although it continued for a further 3 h (Fig. 6c). The difference can be explained by bulky and strongly coordinative triphenylphosphine moieties in the latter structure, which could protect Pd against adsorption onto the resin. Such a behaviour is expected for homogeneous catalysts [23], suggesting that the MNP-based catalysts work as a Pd source, which is released from the support during the reaction.

The strong influence of the scavenger might be explained by a competitive adsorption of Pd species between the MNP and the resin. Considering that the Pd complexes are adsorbed at the surface of MNPs only by physical interactions, much stronger competitive chemical adsorption at the active sites of the resin is plausible. Assuming equilibrium between the adsorbed and low concentrations of free Pd species in solution, the latter can enter the resin pores and be chemisorbed, removing the catalytic function.

3.3. Catalyst performance: kinetic study

The kinetics of Heck coupling of various aryl bromides with n-butyl acrylate or styrene typically gave sigmoidal profiles, with a short induction period as shown in Fig. 7a. The induction period varied with the reaction conditions, after which the reactions followed pseudo-first-order kinetics for at least two orders of magnitude of concentration changes (Fig. 7b). Pseudo-first-order rate constants (k_{obs}) were evaluated from semi-logarithmic concentration–time plots (in all cases $r^2 \geqslant 0.995$) which qualitatively agree with those obtained for conventional homogeneous Pd catalysts described in the literature [20].

3.3.1. Optimisation of catalyst preparation

In our previous work using rhodium catalysts on MNPs, it was found that treatment with ultrasound for 3 h was necessary for quantitative immobilisation of the Rh catalysts onto the surface of MNPs. The same time was used for the preparation of the Pd catalysts used in the initial part of this work. Further study of the immobilisation time was also undertaken for the Pd catalysts. Representative results for Heck reactions catalysed by MNP-[Pd(OAc)$_2$] and MNP-
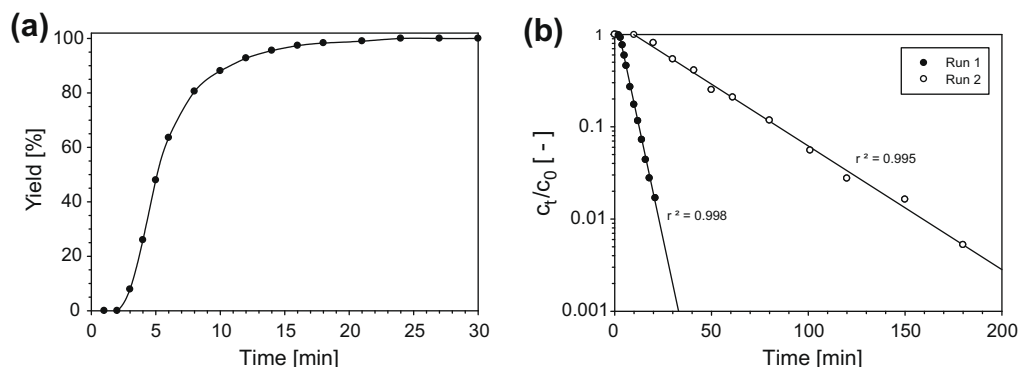

Fig. 7. Heck coupling of 4-bromonitrobenzene with n-butyl acrylate catalysed by MNP-[Pd(OAc)$_2$]: (a) the example of sigmoidal kinetics and (b) the example of pseudo-first-order kinetics. Pd loading (reaction conditions – see Section 2.3.1): (a) 7.5 mol% Pd, (b) Run 1–7.5 mol% Pd, Run 2–2.5 mol% Pd.
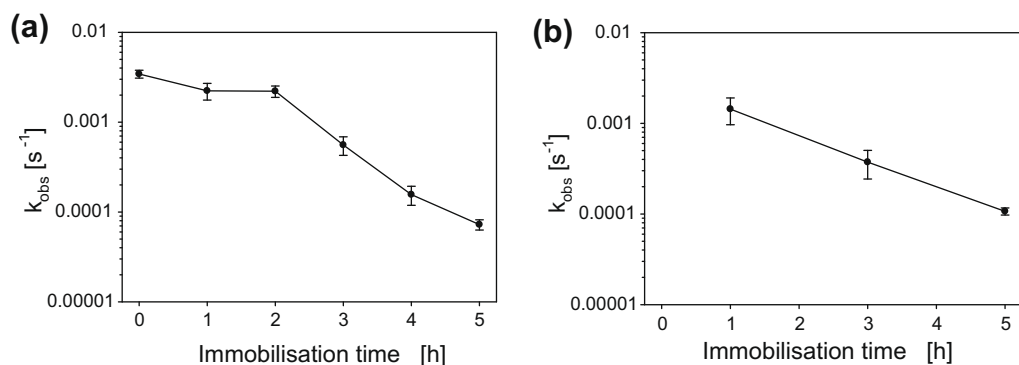

Fig. 8. Catalyst preparation optimisation: effect of ultrasound treatment time on catalyst activity in Heck reaction of 4-bromonitrobenzene with n-butyl acrylate catalysed by (a) MNP-[Pd(OAc)$_2$] and (b) MNP-[Pd(TPP)$_2$(OAc)$_2$].

[Pd(TPP)₂(OAc)₂] are shown in Fig. 8. In all cases reaction was pseudo-first order and the corresponding rate constants were evaluated. For treatment times up to 2 h, the time of US irradiation during the preparation of MNP-[Pd(OAc)₂] had only a small effect on the reaction kinetics. Longer sonication times though reduced the catalytic activity, with the rate constant decreasing by an order of magnitude when the sonication time was increased from 2 to 5 h.

The lowering of catalyst activity for prolonged sonication time could be explained by deactivation of the organometallic palladium through the formation of catalytically inactive palladium black species [16,20c,d]. To investigate any effect of sonication time on catalyst morphology, more detailed studies using high resolution TEM (HRTEM) were undertaken. Comparison of the micrographs for different sonication times revealed the existence of spherical, 3.5 nm diameter Pd particles on the iron oxide support subjected to 3 h sonication, which were not seen in the sample sonicated for 1 h (Fig. 9). The HRTEM image of an individual Pd particle on the surface of the MNP shows an atomic lattice fringe with a distance of 0.2003 nm, which is very close to the lattice spacing of the (2 0 0) Pd(0) lattice plane [25]. Thus, the HRTEM observations together with EDX analysis proved that the prolonged ultrasonic irradiation in the presence of methanol promotes the reduction of Pd ions to colloidal Pd(0) [26]. Although the amount of the reduced palladium is not large, the lower resolution XRD results showed no diffraction peaks corresponding to Pd(0) – the changes in nature and morphology are sufficient to affect the overall catalyst activity. Further experiments showed that changing the sonication time between 1 h and 5 h did not affect the catalyst leaching. Running the reaction on the recovered filtrate after magnetic removal of the catalyst gave 81–89% conversion after 24 h. Where the catalyst was prepared without sonication, 100% conversion was achieved after 12 h indicating that the use of ultrasound results in some degree of anchoring the Pd species onto the MNP surface. Although the exact effect of ultrasound is not clear, it can be concluded that 1 h of sonication is sufficient to give catalysts with higher activity than produced by normal stirring and that longer sonication times are not beneficial. Therefore, in the remaining experiments, catalytic MNPs were prepared using 1 h immobilisation time.

3.3.2. Catalyst loading

The influence of the total amount of catalyst present on the kinetics of the reaction was investigated in two ways: (i) using the same amount of MNPs but changing their loading of Pd(OAc)₂ (between 0.06 and 0.18 mmol Pd per g) and (ii) increasing the number of catalytic MNPs with a fixed loading of 0.12 mmol Pd per g. In all these experiments the immobilisation time used was 1 h of sonication, the results are shown in Fig. 10. For both series of the experiments the increase of catalyst loading increased the observed pseudo-first-order rate constant, k_{obs}, although different effects were seen for the two ways of changing the catalyst concentration.

Simply increasing the number of MNPs added to the reaction has an almost linear effect on k_{obs} (Fig. 10, systems 1–4, white bars) agreeing well with kinetics measurements of C–C coupling for a homogeneous Pd catalysts [20b]. Varying the loading of Pd(OAc)₂ on the MNPs (systems 5, 3 and 6), increased k_{obs} for reactant/Pd ratio from 2.5 to 5 mol% but further increase of the loading 7.5 mol% had little benefit. It is worth noting that the highest catalyst amount (7.5 mol%) was used simply as part of the kinetic study and is not realistic for use in reactions.

The increase of catalyst loading on the MNPs (systems 5, 3 and 6) increases the coverage of organometallic Pd shell; however such changes were not observed in HRTEM analysis. The visible shells of Pd(OAc)₂ were much thinner than the layer of [Rh(TPPMS)(cod)Cl] immobilised on MNPs used by our group previously, where the change of layer thickness for various catalysts' loadings was visible [10].

In discussing the influence of catalyst loading a number of factors related to the catalytic action of immobilised palladium acetate need to be considered: (i) immobilised Pd(OAc)₂ as a source of homogeneous palladium complexes, (ii) heterogeneous catalysis at the outer surface of immobilised Pd(OAc)₂ and (iii) heterogeneous catalysis with possible penetration of reactants into the immobilised organometallic Pd layer. The true picture may be a combination of these.

A solely homogeneous mechanism can be excluded by comparing the rate constants for homogeneous ($k_{obs,h} = 3.25 \times 10^{-3}$ s^{-1}) and MNP-supported Pd(OAc)₂ ($k_{obs,MNPs} = (2.60 \pm 0.04) \times 10^{-3}$ s^{-1}) catalysed reaction of 4-bromonitrobenzene with n-butyl acrylate at 130 °C, a reduction of ca. 20%. It is not realistic to suppose that this amount of Pd would be released from the MNPs during the reaction.

An external surface mechanism can explain the increase of k_{obs} with the increase of catalyst concentration (systems 1–4), and is consistent with the other results shown in Fig. 10. Assuming, following the HRTEM analysis, that the layer of palladium acetate is very thin, the increase of particle number by 50% should increase the accessible surface of catalyst also by 50%. This is in agreement with the obtained values of rate constants ($k_{obs,6} = 2.74 \times 10^{-3}$ s^{-1}, $k_{obs,4} = 3.85 \times 10^{-3}$ s^{-1}; $c_{4\text{-BrPhNO}_2} = 50$ mM, 130 °C); a 41% increase. These results also exclude the possible influence of the "bulk" catalysis–catalysis inside the organometallic layer.

However, comparing systems 2 and 5, the same level of Pd spread over twice the number of MNPs reduces k_{obs} by around 45% ($k_{obs,2} = 0.93 \times 10^{-3}$ s^{-1}, $k_{obs,5} = 0.51 \times 10^{-3}$ s^{-1}). It might be that a thinner layer of immobilised Pd(OAc)₂ did not provide sufficient stabilisation of the dispersion so that aggregation, and hence a decrease of catalyst accessibility, occurred.

3.3.3. Catalyst re-use

The majority of investigations of the repeated use of MNP-based catalysts have only investigated the final conversion after the reac-
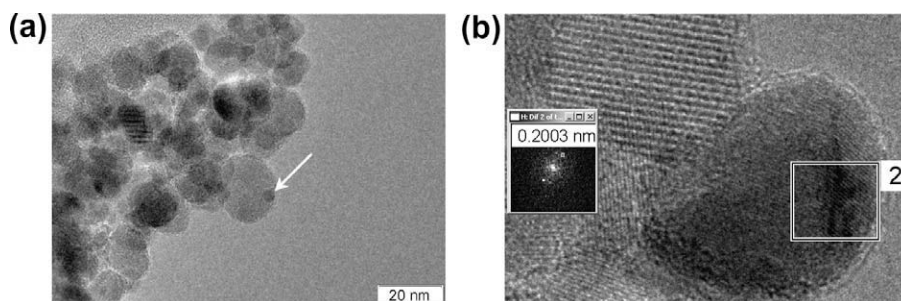

Fig. 9. HRTEM images of MNP-[Pd(OAc)₂] prepared by ultrasonic irradiation for 3 h: (a) the arrow shows spherical Pd(0) nanoparticle of 3.5 nm diameter and (b) Pd(0) nanoparticle lattice.
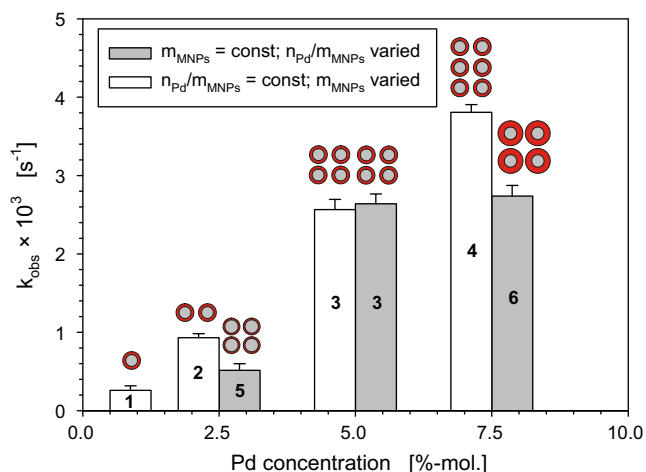
Fig. 10. Catalyst preparation optimisation: effect of palladium loading on catalyst activity in Heck reaction catalysed by MNP-[Pd(OAc)$_2$]. The series for catalyst 3 were repeated twice. m_{MNPs} = mass of magnetic nanoparticles (g), n_{Pd} = moles of Pd (moles). Reaction conditions: 1.0 eq. 4-bromonitrobenzene, 1.2 eq. n-butyl acrylate, 2.0 eq. KOAc, 5 mol% Pd, 10 mL NMP, 130 °C.

tion [5,6,8], an exception being a recent study of hydrodechlorination using Pd(0) which showed that the catalyst lost activity and the rate constant slowed after the first run [27].

In our initial studies (see Table 4), high activity was observed on re-use so that a complete conversion could be achieved on the third or fourth cycle of catalyst use for MNP-[Pd(OAc)$_2$] and MNP-Pd(0) employed in the Heck coupling. However, a detailed investigation of the kinetics of the reaction using MNP-[Pd(OAc)$_2$] indicated pronounced deactivation of the catalyst (Fig. 11) where k_{obs} decreased from 1.7×10^{-3} s^{-1} to 1.1×10^{-5} s^{-1} over the three reaction cycles. Moreover, analysis of the concentration profiles in the repeated experiments showed that the induction period lengthened for consecutive runs. This induction period may correspond to the formation of soluble, active palladium species, during the first, oxidative addition, step of the Heck coupling [20,28]. The results observed for the third re-use of separated and washed MNP-[Pd(OAc)$_2$] showed that the catalyst was still active (see Fig. 11) but, when compared with the fresh catalyst, the reaction was too slow to be of practical use.

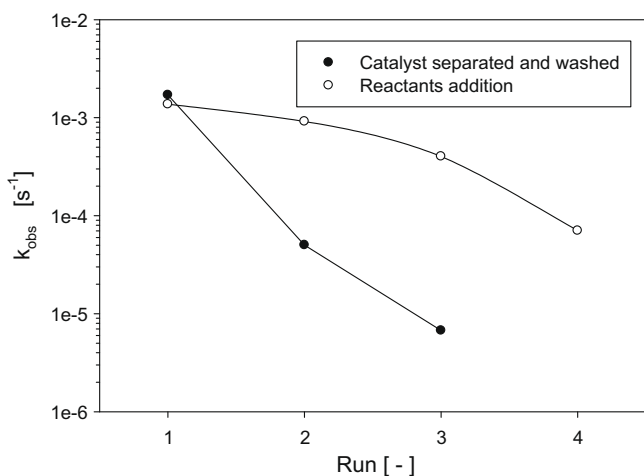Another approach to investigating catalyst deactivation included the addition of aliquots of fresh reactants to the completed reaction mixtures (as monitored by 4-bromonitrobenzene consumption analysed by GC). The activity of MNP-[Pd(OAc)$_2$] decreased with each repeated use of the catalyst, however, as can be seen from Fig. 11, the reaction rate did not decrease to the same extent as when the catalyst was separated from the solution between uses. Under the same conditions as used above, Heck coupling was completed within 100 and 210 min for the second and third additions, respectively. It was also possible to carry out further reaction cycle by adding fresh reactants to the reaction mixture, although the fourth run of Heck coupling occurred with 100% conversion only after 18 h. This may be due to catalyst poisoning by the increasing concentration of reactants and product in solution, although the results suggest that the catalyst may be more suitable for a continuous flow reaction system.

As the second example, the MNP-Pd(0) system was used for the hydrogenation of dimethyl itaconate. Here the examination of the initial reaction rates (Fig. 12) suggests that the catalyst activity maintained at the same level after four reaction cycles. Our results agree with those presented by Panella et al. [29] for asymmetric hydrogenation using a chirally modified Pt/SiO$_2$/Fe$_3$O$_4$ catalyst. The measured rate of Run 3 (the second re-use of the catalyst) is surprisingly low; however, the upper error bars are within the region of uncertainty for the initial rates for all runs (1–4), equal to $(-\mathbf{r}_{AV,0}) = (25.9 \pm 2.2) \times 10^{-3}$ kmol m^{-3} s^{-1} (see Fig. 12, the values of average initial reaction rate and error bars added as lines).

3.3.4. Studies of catalyst stability

To further investigate the observations in the previous section, the potential loss of metal from the MNP was explored. Two parallel syntheses were carried out until the reaction has been completed (as determined by GC) and then the catalyst was magnetically separated: one directly after the reaction while maintaining the process temperature ("hot separation"); the other was first cooled in an ice bath ("cold separation"). The supernatants were checked for Pd content and subsequently used for a Heck reaction after the addition of fresh reactants. In the first approach, the supernatant solution contained 7–9 ppm of Pd was detected in solution by AAS (ca. 5 % of the Pd initially introduced into the reaction flask), whereas no palladium was found after "cold separation". These findings agree well with the mechanism of C–C coupling presented in the literature [20], which includes the presence of soluble palladium species. Additionally, the presence of soluble palladium acetate may result from the shift of adsorption
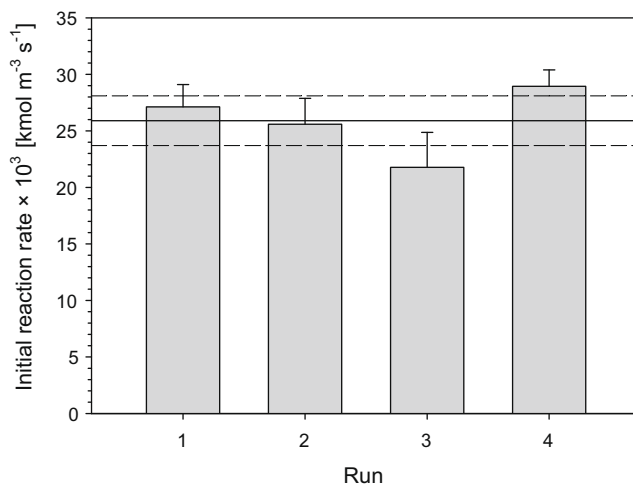

Fig. 11. Kinetic rate constants for MNP-[Pd(OAc)$_2$] catalysed Heck reaction (1.0 eq. 4-bromonitrobenzene, 1.2 eq. n-butyl acrylate, 2.0 eq. KOAc, 5 mol% Pd, 10 mL NMP, 130 °C).

Fig. 12. Initial reaction rates for successive cycles of MNP-Pd(0) catalysed hydrogenation of dimethyl itaconate. Reaction conditions: 0.4 mmol dimethyl itaconate, 1 mol% Pd, 20 mL MeOH, H$_2$ (p = 4 bar), 50 °C.

equilibria at a higher temperature (desorption of $Pd(OAc)_2$), and therefore with some contribution of homogeneously catalysed reaction.

Kinetic investigations of the Heck reaction with residual palladium species gave values of pseudo-first-order rate constants of $k_{obs} = 3.64 \times 10^{-5} \text{ s}^{-1}$ and $k_{obs} = 1.57 \times 10^{-5} \text{ s}^{-1}$ ($c_{4\text{-BrPhNO}_2} = 50$ mM, 130 °C) for "hot" and "cold" separated catalysts, respectively. The fact that AAS analysis showed ca. 7–9 ppm Pd in solution after "hot separation" whereas after "cold separation" the Pd level was <0.1 ppm, suggests that some of Pd species in "hot" solution are catalytically inactive (the ratio of rate constants is ca. 2.3, not two orders of magnitude as Pd concentrations). It might be that some of the leached active metal atoms formed catalytically inactive palladium black [16]. The residual palladium after "cold separation" was sufficient to catalyse subsequent reactions, as previously shown [16a] and this could be one possible explanation for the maintained reactivity after catalyst removal.

In order to determine whether leaching could be caused by the solvent or reactants present in the reaction mixture, MNP-$[Pd(OAc)_2]$ was treated with each of them separately under the reaction conditions (130 °C, NMP). After catalyst removal, the missing reactants were added to the supernatants and the mixtures were immediately used for the standard Heck cross-coupling. The results showed that no reaction occurred after stirring the catalyst with NMP alone, suggesting that there was no soluble active metal after magnetic catalyst separation. Treatment with *n*-butyl acrylate, KOAc and 4-bromonitrobenzene led to a coupling product formation with 4.0%, 33.1% and 60.7% conversion of aryl bromide, respectively, after 24 h of reaction. The corresponding rate constants were equal to $k_{obs} = 1.50 \times 10^{-5} \text{ s}^{-1}$ and $k_{obs} = 5.71 \times 10^{-5} \text{ s}^{-1}$ for KOAc and 4-bromonitrobenzene, respectively. These results show the significant contribution of the presence of aryl halide in the leaching of active species from the nanoparticulate support. It could be explained as a consequence of the oxidative addition of the halide to palladium which leads to the release of Pd(II) into the solution [16,28]. The presence in solution of coordinating acetate groups from the KOAc base could also promote metal leaching.

The "supernatant test" has also been undertaken for the hydrogenation of dimethyl itaconate. Less than 4% conversion for the 24 h long reaction carried out in a homogeneous system after catalyst removal was observed. This result supports the stability of MNP-Pd(0) catalyst as shown in Fig. 12.

4. Conclusion

In conclusion, three MNP-supported palladium systems have been prepared using a novel, straightforward procedure and their activity as catalysts has been investigated. All the catalysts studied exhibited high activity towards C–C bond formation reactions and could be easily separated in a magnetic field and reused for the subsequent recycles. Moreover, the MNP-Pd(0) system promoted the hydrogenation of dimethyl itaconate and selective hydrogenation of benzaldehyde with excellent conversion and selectivity. It has been demonstrated that the organometallic-functionalised catalysts may work as sources for soluble, catalytically active species, which are redeposited onto the nanoparticulate support upon cooling. The results of palladium leaching investigations indicate that the catalyst instability is mainly caused by the presence of aryl bromide. The kinetic screening for catalyst re-use showed loss of activity over each subsequent cycle. We believe that our approach has the potential to show the possible difficulties typically associated with designing of MMNPs-based catalysts, such as catalyst recycling, active metal leaching and system stability.

The kinetic experiments confirmed pseudo-first-order kinetics of Heck reaction also in the case of palladium acetate immobilised on magnetic nanoparticles. Evaluated rate constants were used to optimise the way of organometallic catalyst immobilisation at the surface of MNPs. Detailed kinetic analysis confirmed the deactivation of MNP-$[Pd(OAc)_2]$ in consecutive runs (after magnetic separation).

References

[1] D.J. Cole-Hamilton, Science 299 (2003) 1702.
[2] N.E. Leadbeater, M. Marco, Chem. Rev. 102 (2002) 3217.
[3] I. Angurell, G. Muller, M. Rocamora, O. Rossell, M. Seco, Dalton Trans. (2003) 1194.
[4] (a) D. Astruc, F. Lu, J.R. Aranzaes, Angew. Chem. Int. Ed. 44 (2005) 7852;
(b) R.B. Bedford, M. Betham, D.W. Bruce, S.A. Davis, R.M. Frost, M. Hird, Chem. Commun. (2006) 1398;
(c) B. Berkovski, in: B. Berkovski, V. Bashtovoy (Eds.), Magnetic Fluids and Applications Handbook, Begell House, Inc., New York, Wallingford, 1996, pp. 1–250.
[5] (a) S. Ceylan, C. Friese, Ch. Lammel, K. Mazac, A. Kirschning, Angew. Chem. Int. Ed. 47 (2008) 1;
(b) J. Liu, X. Peng, W. Sun, Y. Zhao, Ch. Xia, Org. Lett. 10 (2008) 3933;
(c) B. Baruwati, D. Guin, S.V. Manorama, Org. Lett. 9 (2007) 5377;
(d) Z. Wang, P. Xiao, B. Shen, N. He, Colloids Surfaces A: Physicochem. Eng. Aspects 276 (2006) 116.
[6] (a) D.K. Yi, S.S. Lee, J.Y. Ying, Chem. Mater. 18 (2006) 2459;
(b) B. Panella, A. Vargas, A. Baiker, J. Catal. 261 (2009) 88;
(c) J. Zhang, Y. Wang, H. Ji, Y. Wei, N. Wu, B. Zuo, Q. Wang, J. Catal. 229 (2005) 114.
[7] V. Polshettiwar, R.S. Varma, Org. Biomol. Chem. 7 (2009) 37.
[8] S. Luo, X. Zheng, J.-P. Cheng, Chem. Commun. (2008) 5719.
[9] V. Polshettiwar, R.S. Varma, Chem. Eur. J. 15 (2009) 1582.
[10] U. Laska, C.G. Frost, P.K. Plucinski, G.J. Price, Catal. Lett. 122 (2008) 68.
[11] T. Suárez, B. Fontal, M. Reyes, F. Bellandi, R.R. Contreras, A. Bahsas, G. León, P. Cancines, B. Castillo, React. Kinet. Catal. Lett. 82 (2004) 317.
[12] J.L. Lyon, D.A. Fleming, M.B. Stone, P. Schiffer, M.E. Williams, Nano Lett. 4 (2004) 719.
[13] Typical experimental capacity 0.19 mmol g^{-1} (based on $Pd(OAc)_2$ in DCM). Commercially available from Sigma Aldrich. <http://www.sigmaaldrich.com>
[14] T. Hyeon, S.S. Lee, J. Park, Y. Chung, H.B. Na, J. Am. Chem. Soc. 123 (2001) 12798.
[15] (a) I.IsmayadimM. Hashim, A.M. Khamirul, R. Alias, Am. J. Appl. Sci. 6 (2009) 1548;
(b) A.W. Burton, K. Ong, T. Rea, I.Y. Chan, Micropor. Mesopor. Mater. 117 (2009) 75 (and literature sited therein).
[16] (a) J.M. Richardson, C.W. Jones, J. Catal. 251 (2007) 80 (and references therein);
(b) V. Farina, Adv. Synth. Catal. 346 (2004) 1553;
(c) A.H.M. de Vries, J.M.C.A. Mulders, J.H.M. Mommers, H.J.W. Henderickx, J.G. de Vries, Org. Lett. 5 (2003) 3285.
[17] J.-P. Corbet, G. Mignani, Chem. Rev. 106 (2006) 2651.
[18] M.B. Smith, J. March, March's Advanced Organic Chemistry, Wiley International, Hoboken, NJ, 2007.
[19] O. Levenspiel, Chemical Reaction Engineering, Wiley, New York, 1999.
[20] (a) D.G. Blackmond, T. Schultz, J.S. Mathew, C. Loew, T. Rosner, A. Pfaltz, Synlett 18 (2006) 3135;
(b) D.G. Blackmond, Angew. Chem. Int. Ed. 44 (2005) 4302;
(c) V. Farina, Adv. Synth. Catal. 346 (2004) 1553;
(d) I.P. Beletskaya, A.V. Cheprakov, J. Organomet. Chem. 689 (2004) 4055;
(e) M. Nowotny, U. Hanefeld, H. van Koningsveld, T. Maschmeyer, Chem. Commun. (2000) 1877.
[21] (a) J. Barluenga, M.A. Fernández, F. Aznar, C. Valdés, Chem. Eur. J. 11 (2005) 2276;
(b) J. Barluenga, M.A. Fernández, F. Aznar, C. Valdés, Chem. Eur. J. 10 (2004) 494;
(c) S.B. Larsen, Tetrahedron 64 (2008) 2938.
[22] V. Polshettiwar, B. Baruwati, R.S. Varma, Chem. Commun. (2009) 1837–1839.
[23] J.M. Richardson, C.W. Jones, Adv. Synth. Catal. 348 (2006) 1207.

    U. Laska et al./Journal of Catalysis 268 (2009) 318–328

[24] (a) F.Y. Zhao, B.M. Bhanage, M. Shirai, M. Arai, Chem. Eur. J. 6 (2000) 8;
(b) L. Djakovitch, M. Wagner, C.G. Hartung, A. Beller, K. Koehler, J. Mol. Catal. A: Chem. 219 (2004) 121;
(c) A.F. Shmidt, L.V. Mametova, Kinet. Catal. 37 (1996) 406;
(d) A. Biffis, M. Zecca, M. Basato, J. Mol. Catal. A: 173 (2001) 249;
(e) N.T.S. Phan, M. Van Der Sluys, C.W. Jones, Adv. Synth. Catal. 348 (2006) 609.
[25] (a) W.B. Pearson, A Handbook of Lattice Spacings and Structures of Metals and Alloys, Pergamon Press, Oxford, 1967;

(b) K.J. Stevens, B. Ingham, M.F. Toney, S.A. Brown, A. Lassesson, Curr. Appl. Phys. 8 (2008) 443.
[26] (a) K. Okitsu, A. Yue, S. Tanabe, H. Matsumoto, Chem. Mater. 12 (2000) 3006;
(b) N. Arul Dhas, H. Cohen, A. Gedanken, J. Phys. Chem. B 101 (1997) 6834.
[27] H. Hildebrand, K. Mackenzie, F.D. Kopinke, Environ. Sci. Technol. 43 (2009) 3254.
[28] C. Amatore, A. Jutand, J. Organomet. Chem. 576 (1999) 254.
[29] B. Panella, A. Vargas, A. Baiker, J. Catal. 261 (2009) 88.